Published in final edited form as:
Stroke. 2008 July ; 39(7): 2085–2090. doi:10.1161/STROKEAHA.107.509422.

Nascent Aneurysm Formation at the Basilar Terminus Induced by Hemodynamics

Ling Gao, PhD[*], **Yiemeng Hoi, PhD**[*], **Daniel D. Swartz, PhD**, **John Kolega, PhD**, **Adnan Siddiqui, PhD, MD**, and **Hui Meng, PhD**

From the Toshiba Stroke Research Center (L.G., Y.H., D.D.S., J.K., A.S., H.M.) and the Departments of Mechanical and Aerospace Engineering (Y.H., H.M.), Neurosurgery (L.G., D.D.S., A.S., H.M.), Pediatrics (D.D.S.), and Pathology & Anatomical Sciences (J.K.), State University of New York at Buffalo, Buffalo, NY

Abstract

Background and Purpose—Hemodynamic insults at arterial bifurcations are hypothesized to play a key role in intracranial aneurysm formation. This study investigates aneurysm-initiating vascular responses at the rabbit basilar terminus subsequent to common carotid artery ligation.

Methods—Nine adult female New Zealand white rabbits were subjected to sham, unilateral, or bilateral common carotid artery ligation to produce varying degrees of compensatory basilar artery flow increase. Basilar artery flow velocity and geometry were monitored by transcranial Doppler and rotational angiography, respectively, for 12 weeks after surgery. Bifurcation tissues were harvested at 12 weeks and examined histologically. From the histological sections, we quantified the destructive structural changes at the basilar terminus and correlated them with the basilar artery flow rate increase.

Results—Subsequent to common carotid artery ligation, basilar artery flow rate increased by 105% to 900% at the maximum. All common carotid artery-ligated rabbits presented nascent aneurysm formation characterized by a bulge with thinned media and absent internal elastic lamina near the basilar terminus. We defined a nascent aneurysm index based on a multiplicative combination of the local destructive remodeling lengths measured at the nascent aneurysm. The nascent aneurysm index strongly correlated with the increase in basilar artery flow rate with R^2=0.91.

Conclusion—Without other known predisposition, flow increase alone at the basilar bifurcation can lead to a nascent aneurysm. This nascent aneurysm formation is dose-dependent on basilar artery flow increase.

Keywords

aneurysm; angiography; basilar artery; hemodynamics; animal model

To understand how intracranial aneurysms (IAs) develop, experimental models allowing elucidation of the causal relationship between hemodynamics and aneurysm are greatly needed. Intracranial aneurysms have been successfully induced in rodents[1-4] and primates.[5] However,

Correspondence to Hui Meng, PhD, Toshiba Stroke Research Center, State University of New York at Buffalo, 447 Biomedical Research Building, 3435 Main Street, Buffalo, NY 14214. E-mail huimeng@buffalo.edu.

[*]L.G. and Y.H. contributed equally to this work.

Disclosures

J.K. is a consultant for Boston Scientific (for a project not directly related to the topic of this article). A.S. is Speaker Honoraria for the American Association of Neurological Surgeons Course and Emergency Medicine Conference. H.M. receives research funding from National Institute of Health and University at Buffalo.

due to the small caliber of intracranial arteries in rodents and the prohibitive complexity of primate research, these experimental models are not ideally suited for evaluation of hemodynamics. A little-cited report in 1963 showed that common carotid artery (CCA) ligation was able to induce a budding aneurysm in rabbit posterior intracranial circulation without any known aneurysm predisposing risk factor within 5 months.[6] It was thus reasoned that the CCA ligation must have caused increased flow and hence increased hemodynamic stresses in the posterior intracranial arteries, which triggered aneurysm initiation.

To quantify detailed hemodynamics related to aneurysm-initiating vascular remodeling, we previously created a canine cervical arterial bifurcation model that consisted of anastomotic CCAs.[7,8] Using 3-dimensional angiography-based computational fluid dynamics and hemodynamics-histology mapping, we demonstrated that hemodynamics in a defined "danger zone" at the bifurcation apex was responsible for destructive remodeling that mimicked aneurysm initiation. Encouraged by this result, we sought to examine a possible causal relationship between hemodynamic insult and aneurysm initiation at intracranial bifurcations. The current study attempts to confirm aneurysm initiation at the rabbit basilar terminus (BT) subsequent to increases in flow and explore dose dependence of increasing flow. We approach this by quantifying both the hemodynamic stimulus and accompanying tissue destruction (ie, aneurysm pathogenesis) and seek a possible correlation between the two.

Methods

Animal Surgery

Adult female New Zealand white rabbits (3 to 4 kg; Harlan Sprague Dawley, Inc) were selected to allow accurate basilar artery (BA) imaging and easy access to transcranial Doppler velocity measurement. The animals were sedated using ketamine and xylazine and then randomly subjected to either unilateral (n=3) or bilateral (n=3) carotid artery ligation through a midline cervical incision to obtain different degrees of flow rate increase in basilar artery (Figure 1). In sham controls (n=3), carotid arteries were exposed but not ligated. All procedures were in accordance with institutional guidelines for animal experimentation and approved by the local Institutional Animal Care and Use Committee.

Imaging

Three-dimensional rotational angiography was performed on post-procedure days 0, 4, 7, 14, 28, 56, and 84 in a Toshiba Medical System (Infinix, Vx-i) angiography suite. Contrast injection was with a 4-Fr sheath in the femoral or central ear artery.

Before this study, we were able to faithfully image tortuous vessels down to 0.38 mm luminal diameter and within 10% accuracy. At 0.7 mm (the smallest basilar artery lumen), the measurement accuracy was within 2%. This was tested by angiographic imaging of contrast-filled winding microcatheters with inner diameters ranging from 0.15 to 0.7 mm. For angiogram size calibration, we placed 2 beads of 4.65 mm diameter on the anesthetized animal (one at the lower jaw bone, the other between the eyes) and imaged them simultaneously with the cerebral vessels. A scaling factor was obtained from the angiographic image of the beads and used to scale the measured vessel sizes at 6 different locations. These steps ensured that the BA diameter measurement was reliable.

Flow Analysis and Hemodynamic Parameters

Transcranial Doppler (Spencer Technology, Seattle, Wash) velocity measurements at the BA were obtained before ligation and on postprocedure days 1, 4, 7, 14, 28, 56, and 84. The transcranial Doppler measurement was blinded to the ligation procedures. Using the measured

velocity and mean BA diameter measured from angiography images, the BA flow rates (Q) were estimated as follows:

$$Q = V \times A, \text{where } V \text{ is velocity and } A \text{ is BA cross-sectional area.}$$

In addition, the percentage change of flow rate was also quantified and defined as

$$\text{Flow Rate Change}\,(\%) = \frac{\text{Max Flow Rate (after ligation)} - \text{Flow Rate (before ligation)}}{\text{Flow Rate (before ligation)}} \times 100\%$$

To check if the rabbits developed hypertension after CCA ligation, we measured their blood pressure with a pressure cuff before and after CCA ligation.

Tissue Preparation

Immediately after euthanasia (100 mg/kg sodium pentobarbital) at 84 days (12 weeks) postligation, the arteries were perfused at 150 mm Hg for 20 minutes with 10% phosphate-buffered formalin. The brain was then carefully removed and fixed in 10% phosphate-buffered formalin for at least 24 hours. Finally, the basilar bifurcations were embedded in paraffin, sectioned longitudinally (4 μm thickness), and stained with van Gieson or trichrome stains.

Statistical Evaluation

All data are represented as mean±SD. Statistical analysis was performed by unpaired t test to compare blood pressure before and after CCA ligation groups and by analysis of variance to compare the flow rate increase among sham control, unilateral, and bilateral groups. Differences were deemed to be significant when $P<0.05$.

Results

Ligation of one or both CCAs caused a compensatory increase in BA flow (Figure 2), augmenting the hemodynamic stresses at the BT. The flow rate in both ligated groups increased considerably from baseline and remained elevated throughout 84 days (Figure 2A). We observed the maximum BA flow rate increase ranging from 105% to 920% in the ligated groups with the bilateral ligation group exhibiting significantly more flow increase than the unilateral ligation group. Sham-operated controls displayed no significant change in the BA flow rate. Analysis of variance demonstrated significant differences in flow rate increase among sham control, unilateral, and bilateral groups. The baseline BA flow rate for individual rabbits and corresponding maximum BA flow rate increase are shown in Figure 2B.

To examine if carotid ligation caused hypertension in the rabbits, we also measured rabbit blood pressure before and after CCA ligation with a pressure cuff. These pressure values were 72±8 mm Hg and 75±10 mm Hg, respectively. The difference between the two was not statistically significant.

Histological staining of the bifurcations at euthanasia revealed that the ligated groups presented with severe, localized vascular disruption near the BT (Figure 3B1-C3). The sham control group appeared similar to unoperated rabbits with intact, continuous internal elastic lamina (IEL; purple arrows in Figures 3A1 and 3A2) and intact media (between purple arrowheads in Figure 3A3) at the BT. The disruption region in the ligated groups was characterized by a nascent bulge (labeled “B” in Figures 3B1 and 3C1) with IEL missing in an extended region (between red arrows in Figures 3B1 and 3C1) and media thinned in the bulge (between red arrowheads in Figures 3B3 and 3C3). The bulges formed in the bilateral group (Figure 3C1-C3) were larger, more distinct, and extending well into the adventitia, whereas the unilateral group only showed a small bulge (Figure 3B1-B3) representing a less advanced nascent aneurysm. The morphology of these bulges was similar to that reported by Hassler for rabbits

subjected to CCA ligation for 1 to 5 months[6] and "early aneurysms" morphology as reported in rat models.[9,10]

To determine if there was a correlation between the aneurysm-initiating destructive remodeling and the hemodynamic insult at the BT, we measured the luminal length along the bulge, the maximum length of the vascular wall exhibiting thinned media, and the maximum length of IEL loss including the bulge (Table) to quantify the degree of local destructive remodeling. These destruction length measurements were blinded to the flow rate increase. For all samples, we chose the maximum disruption length to avoid artificial measurement errors due to the section plane. Each of these destruction lengths, normalized by the preligation BA diameter, exhibited a positive correlation with the flow rate increase (Figure 4A). The product of the three was defined as the nascent aneurysm index (NAI) to reflect the overall degree and severity of destructive remodeling,

$$\mathrm{NAI}=\frac{\text{Bulge Length}\times\text{Media Thinning Length}\times\text{IEL Loss Length}}{(\text{BA Diameter before Ligation})^3}\times 1000.$$

Note that NAI was defined by multiplicative combination of the three so that with any one of them missing, the NAI would be zero, meaning no aneurysm formed. The computed NAI correlated strongly with flow rate increase with R^2=0.91 (Figure 4B).

Discussion

Increased Hemodynamic Insults Can Initiate Nascent Aneurysms

It has been demonstrated that the complex hemodynamic environment at arterial bifurcation is characterized by high wall shear stress (which is a frictional force on the endothelium from blood flow) and high wall shear stress gradient. This unique combination of wall shear stress and wall shear stress gradient at the bifurcation apex is speculated to predispose the local vessel wall to aneurysm initiation.[7,8] Abnormally high flow in intracranial arteries such as the afferent feeding arteries draining into low resistance venous sumps within arteriovenous malformations in patients is believed to increase the incidence of IA.[11] However, the correlation between high flow and aneurysm incidence or the degree of destructive arterial remodeling at the bifurcation apex has not been well established.

The present study, as well as Hassler's 1963 report,[6] demonstrates that in the absence of other known predisposing factors such as hypertension, genetic susceptibility, and vascular wall weakening factors, an increased hemodynamic insult can initiate nascent aneurysms at the rabbit BT. Hassler reported 6 of 20 unilaterally ligated rabbits and both of 2 bilaterally ligated rabbits displayed aneurysms in the posterior circulation over a period of 1 or 5 months after ligation. However, the incidence of aneurysms at each time point was not specified, and the aneurysm morphological changes were not thoroughly quantified. In addition, although "hydraulic imbalance" was suggested to play an important role in aneurysm occurrence,[6] a relationship between increased hemodynamic insult and aneurysm initiation was not verified. Our data indicate that in both ligation groups, blood flow through the BA was substantially increased (by 105% to 920%) to compensate for CCA ligation. This compensatory increase was expected secondary to the patency of the circle of Willis anastomotic channels and the tight coupling of cerebral blood flow to cerebral metabolism and function. Higher flow impingement at a bifurcation apex would result in further elevation of wall shear stress and wall shear stress gradient in the hemodynamic "danger zone." The bifurcation danger zone hemodynamic insult can trigger local maladaptive vascular remodeling leading to aneurysm initiation.[7,8] However, within the duration of this study (12 weeks postligation), it remains inconclusive whether these nascent aneurysms will eventually develop into full-blown, clinically significant aneurysms.

Nascent Aneurysmal Destructive Remodeling Is Dose-Dependent on Increasing Flow

Characteristics such as vascular wall outward bulging, thinning media, and loss of IEL in our rabbit model are consistent with those of early-stage IA found in rodent[2] or primate[5] models, which have been shown to develop (over the long term) into saccular aneurysms similar to human IAs. The concurrence of a bulge, thinned media, and absent IEL not only strongly suggests an aneurysm-like entity, but because all 3 features are measurable, we can quantify the degree of destructive remodeling signifying the nascent aneurysm. Our data indicate that the degree of arterial remodeling represented by the nascent aneurysm at this aneurysm-prone site differed for different amounts of hemodynamic insult. The unilateral group, which exhibited a smaller flow increase than the bilateral group, underwent less destructive remodeling and subsequently reduced nascent aneurysm development. We further confirmed that the NAI strongly correlated with flow increase. This suggests that the likelihood of IA formation improves with increasing hemodynamic insult in a dose-dependent manner. Therefore, it is not unexpected that patients with increased blood flow in the posterior circulation (secondary to concomitant carotid artery occlusion) have higher chances of IAs.[12,13]

We previously reported that aneurysm-like remodeling was localized in regions experiencing a combination of high wall shear stress and high wall shear stress gradient at a surgically created bifurcation apex in a canine model.[7,8] We suspect that endothelial cells at bifurcation apices become dysfunctional under sustained abnormal hemodynamic conditions, thereby triggering local maladaptive responses leading to aneurysm initiation. We expect to use this rabbit model to evaluate specific hemodynamic insult at these aneurysm-prone sites to decipher precise hemodynamic triggers that induce the pathological remodeling response. The underlying molecular signals and pathways that transduce hemodynamics into remodeling also remain to be uncovered.

A Promising Experimental Aneurysm Model

Recent developments in computational fluid dynamics enable detailed characterization of 3-dimensional hemodynamics in large vessels, thus allowing the computed hemodynamics to be correlated with specific tissue responses in local microenvironments.[14] These advanced techniques enable us to study the causal relationship between hemodynamics and underlying IA pathogenesis, which can only be done in an experimental aneurysm animal model. The experimental model should not only capture human IA etiology, but also allow quantification of aneurysmal hemodynamics. However, existing widely used, large-animal aneurysm models fail to capture the human IA etiology. They are artificially and surgically created either by grafting a vein pouch onto an arteriotomy of the carotid artery[15] or by applying elastase onto a distally ligated carotid stump.[16,17] Furthermore, these surgically created pouches are made of extracranial arteries or veins, which differ structurally from their intracranial counterparts. Intracranial arteries only have a prominent IEL, a relatively thin medial layer, and an insignificant adventitia. Such structures make intracranial arteries prone to aneurysm formation once the vascular wall integrity is disrupted.[18] The differences between intracranial and extracranial arteries cannot be overlooked when probing into the pathogenesis and IA natural history. Other experimental model systems use flow modification (eg, CCA ligation) coupled with induced hypertension and/or treatment with β-aminopropionitrile to induce IA in rats,[1-4] mice,[19] and monkeys.[5] Despite histopathologic similarity with human saccular aneurysms, rodent models do not permit accurate characterization of the aneurysmal hemodynamic microenvironment due to small intracranial arterial sizes. Primate models, however, are not practical due to prohibitive cost and handling. These limitations preclude their use in correlating hemodynamics and aneurysm initiation.

The current rabbit aneurysm model shares similar morphological characteristics to the rodent intracranial models at similar early time points[10,19] with the advantages that the rabbit coagulation system is similar to that of humans[20] and rabbit cerebral vessel sizes are accessible by Doppler and angiographic techniques. Although more efforts are needed to compare our nascent aneurysms against true human IA, we believe they capture aneurysm initiation at early stages. More importantly, this model experiences only hemodynamic insults, thereby enabling examination of the precise role of hemodynamics in aneurysm initiation without confounding factors (other risk factors such as hypertension and vessel structural weakness can be introduced in this model in future studies). Taking advantage of image-based computational fluid dynamics, we expect to uncover the exact relationship between local hemodynamics at the BT and the resulting local tissue responses as well as cellular and molecular mechanisms of the flow-induced aneurysm development. Such correlation will open the doors for improved flow-modifying intervention and potentially noninvasive pharmacological intervention in the future.

Conclusion

We have shown that in the absence of known predisposition, drastic flow increases alone can lead to a nascent aneurysm at the BT. This nascent aneurysm formation is dose-dependent on BA flow rate increase. How aneurysmal hemodynamics correlate with the local cellular and molecular responses requires further investigation. The rabbit IA model can potentially be used to study the underlying mechanisms leading to aneurysm initiation.

Acknowledgments

We thank Ann Marie Paciorek and Feng-Chi Chang for assistance in angiography, Markus Tremmel and Jianping Xiang for assistance in transcranial Doppler and diameter measurements, and Petru M. Dinu for assistance in image reconstruction. We gratefully acknowledge stimulating discussions with W. L. Young, support from L. N. Hopkins and Stephen Rudin, and critique from J. Mocco. This material is based on work funded by the National Institutes of Health under Grants NS047242, EB002873, and NS043924 and by the University at Buffalo Interdisciplinary Research Development Fund (IRDF).

References

1. Hashimoto N, Handa H, Hazama F. Experimentally induced cerebral aneurysms in rats. Surg Neurol 1978;10:3–8. [PubMed: 684603]
2. Hashimoto N, Handa H, Hazama F. Experimentally induced cerebral aneurysms in rats: part III. Pathology. Surg Neurol 1979;11:299–304. [PubMed: 441917]
3. Hashimoto N, Handa H, Hazama F. Experimentally induced cerebral aneurysms in rats: part II. Surg Neurol 1979;11:243–246. [PubMed: 473023]
4. Hashimoto N, Handa H, Nagata I, Hazama F. Experimentally induced cerebral aneurysms in rats: part V. Relation of hemodynamics in the circle of Willis to formation of aneurysms. Surg Neurol 1980;13:41–45. [PubMed: 7361257]
5. Hashimoto N, Kim C, Kikuchi H, Kojima M, Kang Y, Hazama F. Experimental induction of cerebral aneurysms in monkeys. J Neurosurg 1987;67:903–905. [PubMed: 3681429]
6. Hassler O. Experimental carotid ligation followed by aneurysmal formation and other morphological changes in the circle of Willis. J Neurosurg 1963;20:1–7. [PubMed: 14184980]
7. Meng H, Swartz DD, Wang Z, Hoi Y, Kolega J, Metaxa EM, Szymanski MP, Yamamoto J, Sauvageau E, Levy EI. A model system for mapping vascular responses to complex hemodynamics at arterial bifurcations in vivo. Neurosurgery 2006;59:1094–1100. [PubMed: 17143243]discussion 1100-1191
8. Meng H, Wang Z, Hoi Y, Gao L, Metaxa E, Swartz DD, Kolega J. Complex hemodynamics at the apex of an arterial bifurcation induces vascular remodeling resembling cerebral aneurysm initiation. Stroke 2007;38:1924–1931. [PubMed: 17495215]

9. Fukuda S, Hashimoto N, Naritomi H, Nagata I, Nozaki K, Kondo S, Kurino M, Kikuchi H. Prevention of rat cerebral aneurysm formation by inhibition of nitric oxide synthase. Circulation 2000;101:2532–2538. [PubMed: 10831529]
10. Kondo S, Hashimoto N, Kikuchi H, Hazama F, Nagata I, Kataoka H. Apoptosis of medial smooth muscle cells in the development of saccular cerebral aneurysms in rats. Stroke 1998;29:181–189. [PubMed: 9445349]
11. Redekop G, TerBrugge K, Montanera W, Willinsky R. Arterial aneurysms associated with cerebral arteriovenous malformations: classification, incidence, and risk of hemorrhage. J Neurosurg 1998;89:539–546. [PubMed: 9761046]
12. Fujiwara S, Fujii K, Fukui M. De novo aneurysm formation and aneurysm growth following therapeutic carotid occlusion for intracranial internal carotid artery (ICA) aneurysms. Acta Neurochir (Wien) 1993;120:20–25. [PubMed: 8434512]
13. Yousaf I, Gray WJ, McKinstry CS, Choudhari KA. Development of posterior circulation aneurysm in association with bilateral internal carotid artery occlusion. Br J Neurosurg 2003;17:471–472. [PubMed: 14635758]
14. Hassan T, Timofeev EV, Saito T, Shimizu H, Ezura M, Matsumoto Y, Takayama K, Tominaga T, Takahashi A. A proposed parent vessel geometry-based categorization of saccular intracranial aneurysms: computational flow dynamics analysis of the risk factors for lesion rupture. J Neurosurg 2005;103:662–680. [PubMed: 16266049]
15. Spetzger U, Reul J, Weis J, Bertalanffy H, Thron A, Gilsbach JM. Microsurgically produced bifurcation aneurysms in a rabbit model for endovascular coil embolization. J Neurosurg 1996;85:488–495. [PubMed: 8751637]
16. Miskolczi L, Guterman LR, Flaherty JD, Hopkins LN. Saccular aneurysm induction by elastase digestion of the arterial wall: a new animal model. Neurosurgery 1998;43:595–600. [PubMed: 9733315]discussion 600-691
17. Cloft HJ, Altes TA, Marx WF, Raible RJ, Hudson SB, Helm GA, Mandell JW, Jensen ME, Dion JE, Kallmes DF. Endovascular creation of an in vivo bifurcation aneurysm model in rabbits. Radiology 1999;213:223–228. [PubMed: 10540666]
18. Schievink WI. Intracranial aneurysms. N Engl J Med 1997;336:28–40. [PubMed: 8970938]
19. Morimoto M, Miyamoto S, Mizoguchi A, Kume N, Kita T, Hashimoto N. Mouse model of cerebral aneurysm: experimental induction by renal hypertension and local hemodynamic changes. Stroke 2002;33:1911–1915. [PubMed: 12105374]
20. Heilman CB, Kwan ES, Wu JK. Aneurysm recurrence following endovascular balloon occlusion. J Neurosurg 1992;77:260–264. [PubMed: 1625015]

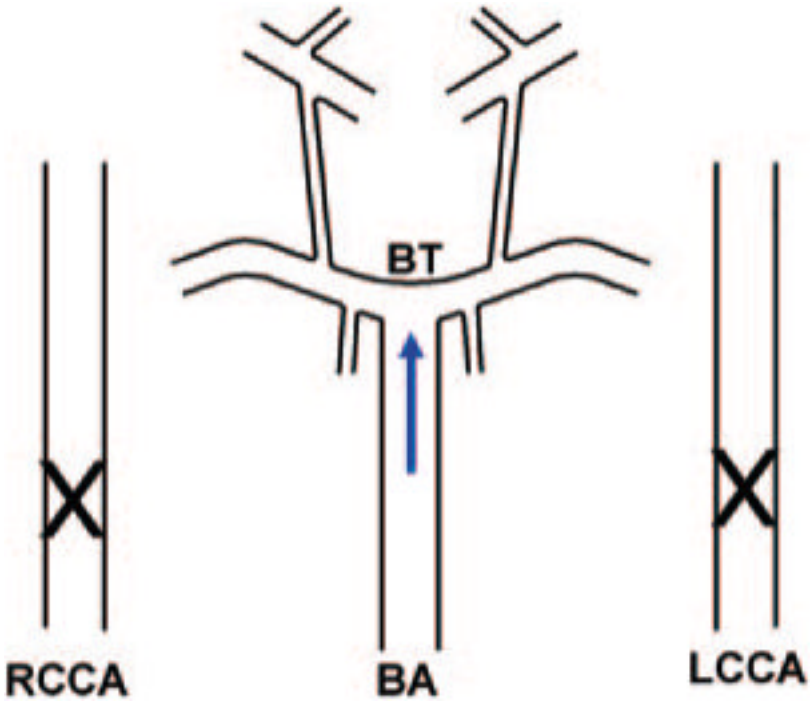

Figure 1.
Schematic diagram for nascent aneurysm induction at rabbit BT through CCA ligation. RCCA indicates right CCA; BA, basilar artery; LCCA, left CCA. In the unilateral ligation group, LCCA was left open.

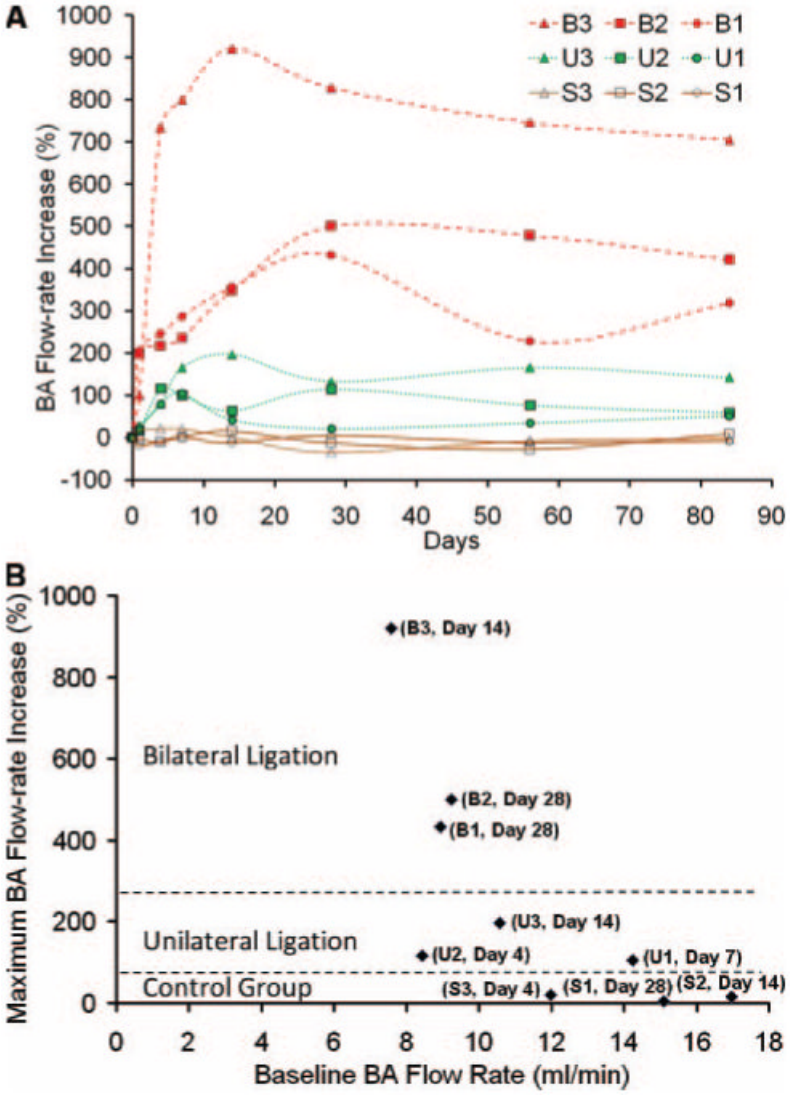

Figure 2.

BA flow rate increase postprocedure. A, Flow rate increase over time in individual rabbits. B, Maximum flow rate increase and corresponding baseline flow rate for individual rabbits. Number of days to achieve maximum flow rate increase is indicated in parentheses.

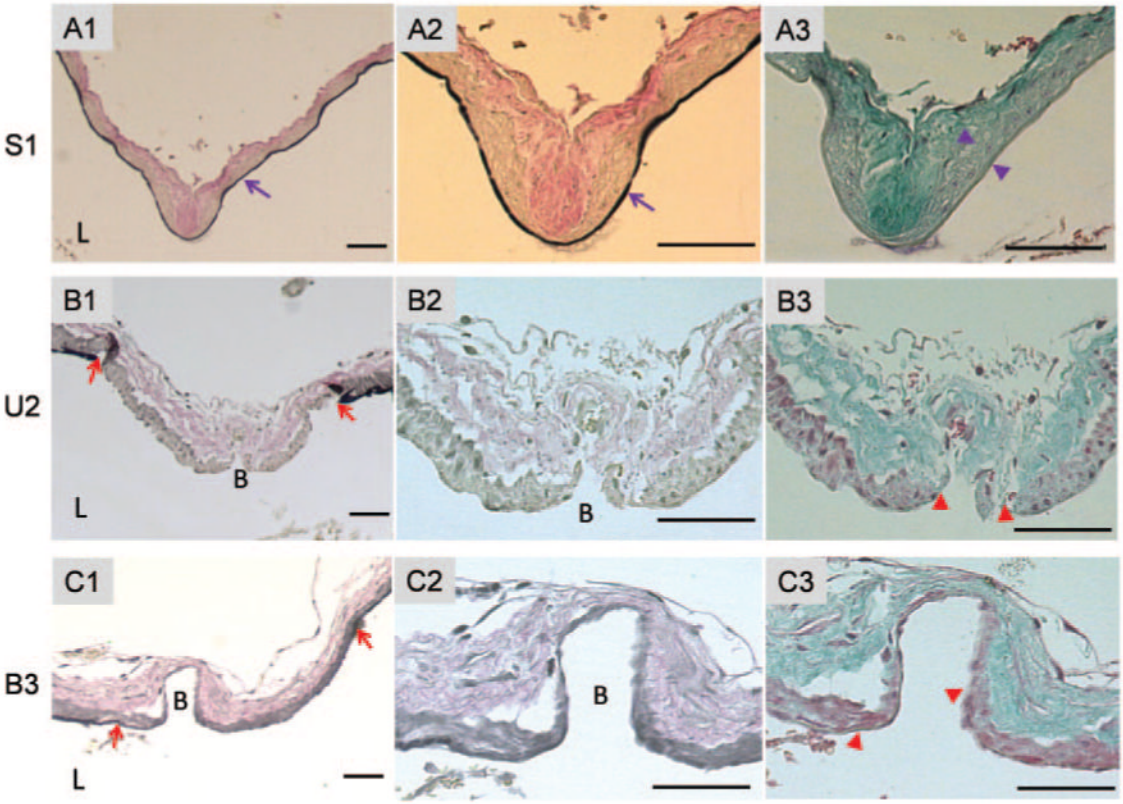

Figure 3.

Nascent aneurysm morphology at BT at 84 days (12 weeks) postprocedure. The second and third columns show higher magnification of the apex at the BT. Top row (A1-A3), sham control (rabbit S1). Continuous IEL (purple arrow in A1 and A2) and intact media (between purple arrowheads in A3) are observed. Second row (B1-B3), unilateral ligation (rabbit U2). Bottom row, bilateral ligation (rabbit B3). The ligation groups exhibit loss of IEL (between red arrows in B1 and C1) and thinned media (between red arrowheads in B3 and C3). A1-A2, B1-B2, and C1-C2, Van Gieson staining showing elastin. A3, B3, and C3, trichrome staining showing collagen and cells. Bar=50 μm. L indicates lumen. B=Bulge.

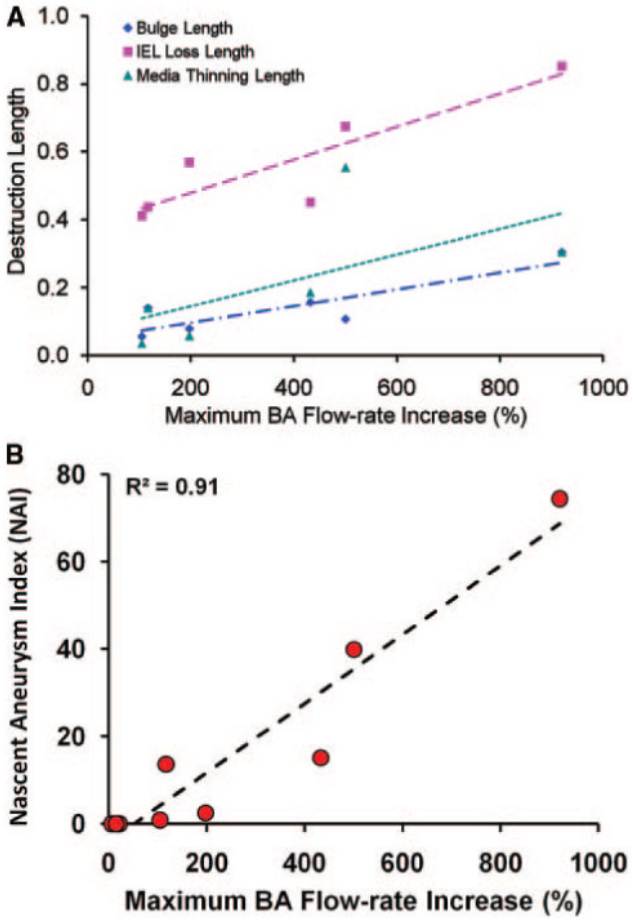

Figure 4.

A, Individual maximum destruction lengths at BT, normalized by the rabbit BA diameter, versus maximum BA flow rate increase in the ligated rabbits. B, NAI, a composite that measures the degree of destructive remodeling, shows strong correlation with percentage of BA flow rate increase.

Table

Flow and Morphological Measurements of Nascent Aneurysms

Rabbits	BA Flow Rate Increase, %	Bulge Length, μm	Media Thinning Length, μm	IEL Loss Length, μm	NAI
Sham					
S1	5	0	0	0	0
S2	15	0	0	0	0
S3	21	0	0	0	0
Ligation (unilateral)					
U1	105	50	32	370	0.8
U2	117	105	105	525	13.7
U3	197	55	40	398	2.6
Ligation (bilateral)					
B1	432	120	135	321	15.2
B2	500	75	387	472	39.9
B3	920	213	201	596	74.4